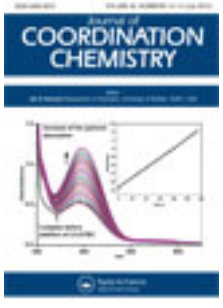

Journal of Coordination Chemistry
Publication details, including instructions for authors and subscription information:
http://www.tandfonline.com/loi/gcoo20

Synthesis and spectroscopic characterization of new heteroleptic ruthenium(II) complexes incorporating 2-(2′-pyridyl)quinoxaline and 4-carboxy-2-(2′-pyridyl)quinoline

Athanassios Philippopoulos [a], Polycarpos Falaras [b], Evagelia Chatzivasiloglou [b c], Olga Igglessi-Markopoulou [c], Vlassis Likodimos [b] & Georgia-Chari Konti [a b]

[a] Faculty of Chemistry, School of Sciences, National and Kapodistrian University of Athens, Athens 15771, Greece

[b] Institute of Physical Chemistry, NCSR "Demokritos", Athens 15310, Greece

[c] Department of Chemical Sciences, School of Chemical Engineering, National Technical University of Athens, Athens 15780, Greece

Accepted author version posted online: 31 May 2012.Published online: 14 Jun 2012.

To cite this article: Athanassios Philippopoulos, Polycarpos Falaras, Evagelia Chatzivasiloglou, Olga Igglessi-Markopoulou, Vlassis Likodimos & Georgia-Chari Konti (2012) Synthesis and spectroscopic characterization of new heteroleptic ruthenium(II) complexes incorporating 2-(2′-pyridyl)quinoxaline and 4-carboxy-2-(2′-pyridyl)quinoline, Journal of Coordination Chemistry, 65:14, 2535-2548, DOI: 10.1080/00958972.2012.698735

To link to this article: http://dx.doi.org/10.1080/00958972.2012.698735

Journal of Coordination Chemistry
Vol. 65, No. 14, 20 July 2012, 2535–2548

Synthesis and spectroscopic characterization of new heteroleptic ruthenium(II) complexes incorporating 2-(2′-pyridyl) quinoxaline and 4-carboxy-2-(2′-pyridyl)quinoline

ATHANASSIOS PHILIPPOPOULOS*†, POLYCARPOS FALARAS‡, EVAGELIA CHATZIVASILOGLOU‡§, OLGA IGGLESSI-MARKOPOULOU§, VLASSIS LIKODIMOS‡ and GEORGIA-CHARI KONTI†‡

†Faculty of Chemistry, School of Sciences, National and Kapodistrian University of Athens, Athens 15771, Greece
‡Institute of Physical Chemistry, NCSR "Demokritos", Athens 15310, Greece
§Department of Chemical Sciences, School of Chemical Engineering, National Technical University of Athens, Athens 15780, Greece

(*Received 2 February 2012; in final form 9 April 2012*)

Starting from *cis*-[Ru(dcbpyH$_2$)$_2$Cl$_2$] (**1**), two new heteroleptic ruthenium(II) complexes, [Ru(dcbpyH$_2$)$_2$(L^1)](NO$_3$)$_2$ (L^1 = 2-(2′-pyridyl)quinoxaline (**2**), and [Ru(dcbpyH$_2$)$_2$(L^2)](NO$_3$)$_2$ (L^2 = 4-carboxy-2-(2′-pyridyl)quinoline (**4**); dcbpyH$_2$ = 2,2′-bipyridine-4,4′-dicarboxylic acid), were synthesized and spectroscopically characterized. During the preparation of **2** and **4**, the homoleptic [Ru(dcbpyH$_2$)$_3$]Cl$_2$ complex (**3**) was isolated as a side product. Characterization includes IR and Raman spectroscopy, UV-Vis, multinuclear NMR spectroscopy, elemental, and ESI-mass spectrometric analyses.

Keywords: 2-(2′-Pyridyl)quinoxaline; 4-Carboxy-2-(2′-pyridyl)quinoline; 2,2′-Bipyridine-4, 4′-dicarboxylic acid; Heteroleptic ruthenium(II) complexes; Spectroscopic characterization

1. Introduction

Coordination chemistry of ruthenium has presented tremendous development for the interesting chemical properties they exhibit [1]. Ruthenium(II) polypyridyl complexes constitute a special category according to their redox, photophysical, and photochemical properties [2]. This class of compounds has been incorporated in solar energy harvesting devices. The discovery of the optoelectronic properties of $[Ru(bpy)_3]^{2+}$ (bpy = 2,2′-bipyridine) [3] has stimulated intense research, where a landmark was the development of dye sensitized solar cells (DSSCs) by Grätzel and co-workers [4] with a ruthenium(II)-coordinated compound (molecular sensitizer or dye) constituting the most critical part of the cell. One of the best sensitizers is *cis*-[Ru(dcbpyH$_2$)$_2$(NCS)$_2$], abbreviated as N3 dye [5]. A series of Ru(II) dyes were developed and tested in the

*Corresponding author. Email: atphilip@chem.uoa.gr

ISSN 0095-8972 print/ISSN 1029-0389 online © 2012 Taylor & Francis
http://dx.doi.org/10.1080/00958972.2012.698735

sensitization of nanocrystalline titania [6]. Ruthenium(II) complexes incorporating phosphine ligands are efficient catalysts in a plethora of organic reactions such as hydrogenation [7], oxidation [8], hydroformylation [9], and homogeneous catalyzed transfer hydrogenations [10].

Ruthenium(II) polypyridyl compounds have potential application as photo-probes for DNA [11], DNA photo-cleavage reagents [12], molecular light switches [13], etc., as possible anticancer reagents [14]. Taking into consideration the importance of ruthenium compounds in such different scientific domains, we have made systematic efforts to prepare appropriate molecular compounds and examine their properties, aiming at possible biological effects [15]. We report herein the syntheses and complete spectroscopic characterization of two new heteroleptic ruthenium(II) complexes, *cis*-$[Ru(dcbpyH_2)_2(L^1)](NO_3)_2$ (**2**) and *cis*-$[Ru(dcbpyH_2)_2(L^2)](NO_3)_2$ (**4**). Their molecular structure comprises the *cis*-$[Ru(dcbpyH_2)_2]^{2+}$ core differing in the nature of the incoming ancillary bidentate ligands L^1 and L^2 (L^1 is 2-(2′-pyridyl)quinoxaline, while L^2 is 4-carboxy-2-(2′-pyridyl)quinoline (scheme 1)).

2. Experimental

2.1. *Materials and methods*

$RuCl_3 \cdot 3H_2O$ (Aldrich), 2,2′-bipyridine-4,4′-dicarboxylic acid (Dyesol Australia), and all other reagents were used as received. Reagent grade solvents were thoroughly degassed by bubbling argon for 15 min prior to use. The starting materials 2-(2′-pyridyl)quinoxaline (L^1) [16], 4-carboxy-2-(2′-pyridyl)quinoline (L^2) [17], and *cis*-$[Ru(dcbpyH_2)_2Cl_2]$ [18] (**1**) were prepared according to the literature methods. All reactions (unless otherwise noted) were carried out under argon by standard Schlenk techniques. The C, H, and N determinations were carried out at the elementary analyses laboratory of the Service Central d′ Analyse (USR-59/CNRS/France). Infrared spectra were measured on a Perkin Elmer 283 spectrometer as KBr pellets from 4000 to 400 cm^{-1}. Micro-Raman spectra were measured in the backscattering configuration using a Renishaw inVia Reflex microscope with an Ar^+ ion laser ($\lambda = 514.5$ nm) as an excitation source. The backscattered Raman light is detected on a high sensitivity, UV-coated, deep depletion CCD detector, while a 50 × objective on a Leica DMLM microscope is used to focus the laser light to a spot size of about 1.5 μm. In all cases, very low laser power density (~5 μW μm^{-2}) was used in order to avoid overheating the compounds. The frequency shifts were calibrated against an internal Si reference. Luminescence background has been subtracted by cubic spline interpolation routines, while spectral deconvolution has been carried out by non-linear least square fitting of the Raman peaks to a mixture of Lorentzian and Gaussian line shapes.

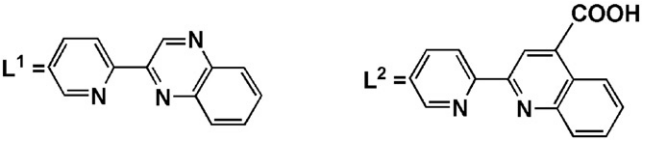

Scheme 1. Structural formulas of L^1 and L^2.

Melting or decomposition points were determined using an Electrothermal 9100 (IA9000 series) digital melting point apparatus and are uncorrected. The samples were sealed in capillary tubes and heated slowly until the compounds melted or decomposed. Absorption spectra were recorded on Perkin-Elmer Lambda 19 and CARY 3E UV-Vis spectrometers. All NMR spectra were recorded at 298 K (Bruker Avance 500 MHz and Varian 300 MHz spectrometers) in D_2O containing NaOD 0.05 mol L^{-1} solution. The ^1H and $^{13}C\{^1H\}$ NMR signals of 2,2′-bipyridine-4,4′-dicarboxylic acid, 2-(2′-pyridyl)-quinoxaline and 4-carboxy-2-(2′-pyridyl)quinoline ligands in **2** and **4** were assigned by H,H-COSY, H,H-NOESY, H,H-ROESY, and H,C-HSQC experiments. Electrospray mass spectra (ESI-MS) were performed on a TSQ 7000 Finnigan Mat spectrometer at the Mass Spectrometry and Dioxin Analysis Lab of the National Centre for Scientific Research "Demokritos."

2.2. *Syntheses*

During all synthetic procedures, light exposure was carefully avoided in order to avoid *cis-trans* isomerization of *cis*-$[Ru(dcbpyH_2)_2Cl_2]$ [19]. The UV-Vis absorption spectrum of the starting material *cis*-$[Ru(dcbpyH_2)_2Cl_2]$ (**1**) in the reaction mixture was recorded showing three absorptions at 318, 429, and 587 nm, while the ratio of the relative intensities of these maxima was approximately 3.85/1/1.08, respectively. The progress of the reaction was monitored by UV-Vis spectroscopy by observing the shift of the three absorptions at 318, 429, and 587 nm and the corresponding intensities of these maxima. After the addition of $AgNO_3$, an aliquot of the reaction mixture was sampled and diluted in DMF. The absorption spectrum displayed a maxima at 318, 392, and 535 nm and the reaction was completed when the ratio of these maxima was 3.29/1.07/1. An equivalent amount of L^1 (**2**) or L^2 (**4**) was added to the non-isolated intermediate and the absorption spectrum was recorded to insure completion of the reaction. A small aliquot of the reaction mixture was sampled and diluted with ethanol. The reaction was stopped until no changes (in the UV-Vis spectra) were observed and when the relative intensities of the absorption spectrum maxima of **2** (at 308, 449, 510 nm) and of **4** (at 310, 344 (sh) and 469 nm) has reached 5.69/1/1 and 4.21/1.40/1 ratios, respectively.

2.2.1. Synthesis of *cis*-$[Ru(dcbpyH_2)_2(L^1)](NO_3)_2$ (2). In a 50 mL round-bottomed flask, **1** (0.180 g, 0.273 mmol) was dissolved in DMF (20 mL), giving a black-green solution. Two equivalents of $AgNO_3$ (0.093 g, 0.547 mmol) were added and the color of the solution changed rapidly to dark violet. The reaction mixture was heated at 60°C for 1 h and was then stirred overnight at an ambient temperature to ensure the completion. The AgCl precipitated was filtered and subsequently centrifuged. To the resulting clear filtrate, 0.057 g (0.273 mmol) of L^1 was added in small portions and the mixture was heated at 120°C. During the course of the reaction, the color of the solution turned dark orange-brown. After 3 h of heating, the reaction mixture was cooled at an ambient temperature and was filtered leaving 84 mg of $[Ru(dcbpyH_2)_3]Cl_2$ (**3**). The volume of the filtrate was subsequently reduced to a few milliliters and an orange-brown solid was precipitated by the addition of acetone (20 mL). The resulting solid was filtered off and dissolved in ethanol (30 mL). The solvent was evaporated to a small amount and the product was precipitated with ether in excess. The orange-brown solid was filtered, thoroughly washed with acetone (2×5 mL) and diethylether (2×10 mL), and finally

was dried *in vacuo*. Yield: 34.4 mg (14%). m.p: >215°C (dec). Anal. Calcd for **2** $2H_2O \cdot (CH_3)_2CO$, $C_{40}H_{35}N_9O_{17}Ru$ (%), C, 47.34; H, 3.48; N, 12.42. Found (%): C, 47.20; H, 3.10; N, 12.05. IR (KBr, $\tilde{\nu}$ in cm^{-1}): 3105 (w, C−H aromatic), 3080 (w, C−H aromatic), 1719 (s, ν(C=O)), 1618 (m), 1546 (m), 1476 (w), 1431 (m), 1405 (s), 1385 (vs, $\nu_{as}(NO_3^-)$), 1317 (s), 1263 (s), 1232 (s, ν(C−O), 1143 (w), 1022 (w), 901 (w), 771 (m), 750 (w), 719 (w), 670 (w), 630 (w), 552 (w). Raman (r.t., cm^{-1}): 1611 (m, ν(C=C)), 1602 (m), 1541 (m), 1533 (s), 1476 (vs), 1363 (s, $\nu_{as}(NO_3^-)$), 1342 (m, w(C−H)), 1300 (m), 1266 (m), 1241 (w), 1166 (w), 1121 (w), 1040 (w), 1026 (w). ^{1}H-NMR (NaOD 0.05 M, 500 MHz, 298 K): δ (ppm) = 9.76 (s, 1H, H_3), 8.94 (s, 1H, $H_{25'}$), 8.92 (s, 1H, H_{25}), 8.87 (d, ^3J(H,H) = 8.08 Hz, 1H, H_{13}), 8.72 (s, 1H, H_{19}), 8.63 (s, 1H, $H_{19'}$), 8.16 (t, ^3J(H,H) = 7.87 Hz, 1H, H_{14}), 8.06 (m, 3H, $H_{6,22,28'}$), 7.75 (m, 4H, $H_{7,16,21,28}$), 7.62 (d, ^3J(H,H) = 5.54 Hz, 1H, H_{27}), 7.54 (m, 3H, $H_{21',22',27'}$), 7.43 (t, ^3J(H, H) = 6.58 Hz, 1H, H_{15}), 7.38 (t, ^3J(H,H) = 7.75 Hz, 1H, H_8), 7.29 (d, ^3J(H,H) = 8.78 Hz, 1H, H_9). ^{13}C-NMR (NaOD 0.05 M, 125.8 MHz, 298 K): δ (ppm) = 170.20 (CO), 170.08 (CO), 170.04 (CO), 169.97 (CO), 156.68 (Cq), 156.63 (Cq), 156.57 (Cq), 156.41 (Cq), 155.82 (Cq), 153.32 (Cq), 152.97 (C_{22} or $C_{28'}$), 151.52 (CH), 151.29 (CH), 151.03 (C_{22} or $C_{28'}$), 150.66 (CH), 145.75 (Cq), 145.61 (Cq), 145.36 (Cq), 145.17 (Cq), 143.64 (Cq), 141.95 (C_3), 141.61 (Cq), 137.72 (C_{14}), 132.16 (C_7), 131.81 (C_8), 129.03 (C_6), 127.43 (C_{15}), 126.03 (3C, $C_{13,27}$, CH), 125.67 (CH), 125.53 (CH), 124.20 (C_9), 123.07 (2C, $C_{25,25'}$), 122.81 (C_{19}), 122.32 ($C_{19'}$). UV-Vis (ε ($(mol\,L^{-1})^{-1}\,cm^{-1}$)): λ_{max} (MeOH, nm) = 491 (11340), 448 (14070), 369 (sh) (13540), 351 (sh) (17450), 307 (56270). ES-MS, +Q1MS mode (MeOH}): *m*/*z* (%) = 398.6 ({M/2}$^{2+}$, 34), 245.2 ({dcbpH$_2$ + H}$^+$, 100), 208.2 ({L^1 + H}$^+$, 50), 201.0 (22), 184.0 (24), 176.3 (52), 158.3 ({dcbpH$_2$ + H − 2CO$_2$}$^+$, 21).

2.2.2. Synthesis of *cis*-[Ru(dcbpyH$_2$)$_2$(L^2)](NO$_3$)$_2$ (4). In a 50 mL round-bottomed flask, **1** (0.057 g, 0.086 mmol) was dissolved in DMF (4 mL). Two equivalents of $AgNO_3$ (0.029 g, 0.172 mmol) were added and the color of the solution changed instantly from black-green to dark violet. The precipitate of AgCl was separated by centrifugation and to the resulting clear filtrate 0.022 g (0.086 mmol) of L^2 was introduced. The resulting mixture was subsequently heated at 55°C for approximately 63 h. During the reaction, the color of the solution turned gradually to dark orange-brown. After cooling at room temperature, the reaction mixture was filtered from 23 mg of insoluble $[Ru(dcbpyH_2)_3]Cl_2$ (**3**). The volume of the filtrate was reduced to a few milliliters and an orange-brown solid was precipitated with acetone (20 mL). The precipitate was dissolved in EtOH (30 mL), concentrated to a few milliliters, and was precipitated with ether (excess). The orange-brown solid was thoroughly washed with acetone (2 × 5 mL) and ether (2 × 10 mL) and was subsequently dissolved in DMF (5 mL). Again the solid was precipitated by the addition of acetone (in excess), washed with acetone (2 × 10 mL) and ether (2 × 5 mL) to afford 12.4 mg of **4** after drying *in vacuo*. Yield: (28%). m.p: 200°C (dec). Anal. Calcd for **4** $\cdot 2H_2O \cdot (CH_3)_2CO$, $C_{42}H_{36}N_8O_{19}Ru$ (%): C, 47.69; H, 3.43; N, 10.59. Found (%): C, 47.26; H, 2.98; N, 9.89. IR (KBr, $\tilde{\nu}$ in cm^{-1}): 3109 (w, C−H aromatic), 3077 (w, C−H aromatic), 1718 (s, ν(C=O), 1616 (m), 1544 (m), 1478 (w), 1431 (m), 1405 (s), 1385 (vs, $\nu_{as}(NO_3^-)$), 1315 (m), 1263 (m), 1232 (m, ν(C−O), 1144 (w), 1022 (w), 900 (w), 771 (m), 679 (w). Raman (r.t., cm^{-1}): 1614 (m, ν(C=C)), 1547 (s), 1481 (vs), 1357 (s, $\nu_{as}(NO_3^-)$, 1341 (m, w(C−H)), 1295 (w), 1269 (m), 1167 (w), 1125 (w), 1026 (m), 905 (w). ^{1}H-NMR (NaOD 0.05 M, 500 MHz, 298 K): δ (ppm) = 8.98 (s, 1H, $H_{25'}$), 8.95 (s, 1H, H_{25}), 8.69 (m, 2H, $H_{13,19}$), 8.59 (s, 1H, $H_{19'}$), 8.46 (s, 1H, H_3),

8.27 (d, ^3J(H,H) = 5.84 Hz, 1H, $H_{22'}$), 8.10 (m, 2H, $H_{14,22}$), 8.03 (d, ^3J(H,H) = 8.16 Hz, 1H, H_6), 7.76 (d, ^3J(H,H) = 5.86 Hz, 1H, $H_{28'}$), 7.72 (d, ^3J(H,H) = 5.79 Hz, 1H, H_{21}), 7.65 (d, ^3J(H,H) = 5.84 Hz, 2H, $H_{16,28}$), 7.57 (m, 3H, $H_{21',27',27}$), 7.50 (t, ^3J(H,H) = 7.60, 1H, H_7), 7.40 (d, ^3J(H,H) = 8.94 Hz, 1H, H_9), 7.35 (t, ^3J(H,H) = 6.27 Hz, 1H, H_{15}), 7.21 (t, ^3J(H,H) = 7.87 Hz, 1H, H_8). $^{13}C\{^1H\}$-NMR (NaOD 0.05 M, 125.8 MHz, 298 K): δ (ppm) = 173.00 (C=O), 170.47 (C=O), 170.31 (C=O), 170.25 (C=O), 170.22 (C=O), 158.22 (Cq), 157.73 (Cq), 156.98 (Cq), 156.80 (Cq), 156.73 (2C, Cq), 153.38 ($C_{22'}$), 151.66 ($C_{28'}$), 151.08 (C_{16} or C_{28}), 150.89 (C_{22}), 150.40 (C_{16} or C_{28}), 149.34 (Cq), 147.59 (Cq), 145.22 (Cq), 145.04 (Cq), 144.88 (Cq), 144.61 (Cq), 137.55 (C_{14}), 130.93 (C_8), 128.61 (C_7), 126.72 (C_{15}), 126.28 (C_6), 125.74 (3C, $C_{21,21',27'}$), 125.56 (C_{13}), 125.37 (C_{27}), 124.89 (C_9), 124.34 (Cq), 122.89 (2C, $C_{25,25'}$), 122.45 (C_{19}), 122.02 ($C_{19'}$), 115.38 (C_3). UV-Vis (ε (mol L^{-1} $^{-1}$ cm^{-1})): λ_{max} (MeOH, nm) = 466 (16050), 344 (sh) (16280), 307 (58260). ES-MS, +Q1MS mode (MeOH): m/z (%) = 433.4 (37), 420.0 ($\{M/2\}^{2+}$, 48), 251.2 ($\{L^2 + H\}^+$, 100), 245.2 ($\{dcbpH_2 + H\}^+$, 76), 207.2 ($\{L^2 + H - CO_2\}^+$, 24).

3. Results and discussion

3.1. *Synthesis*

Complexes **2** and **4** were conveniently synthesized by a two-step procedure. In the first step the precursor *cis*-[Ru(dcbpyH$_2$)$_2$Cl$_2$] (**1**) was prepared by the reaction of $RuCl_3 \cdot 3H_2O$ with dcbpyH$_2$ ligand in refluxing DMF (scheme 2). In the second step, a one-pot reaction [20], treatment of **1** with two equivalents of $AgNO_3$ in the same solvent is accompanied by the precipitation of a white solid (AgCl). Subsequent addition of an equivalent of L^1 or L^2 afforded the heteroleptic cationic complexes *cis*-[Ru(dcbpyH$_2$)$_2$(L^1)](NO$_3$)$_2$ (**2**) and *cis*-[Ru(dcbpyH$_2$)$_2$(L^2)](NO$_3$)$_2$ (**4**) [21] in a pure form, as red-brown microcrystalline solids in 14% and 28% yield, respectively, after repeated crystallizations of the mother liquor (scheme 3). They are quite stable and

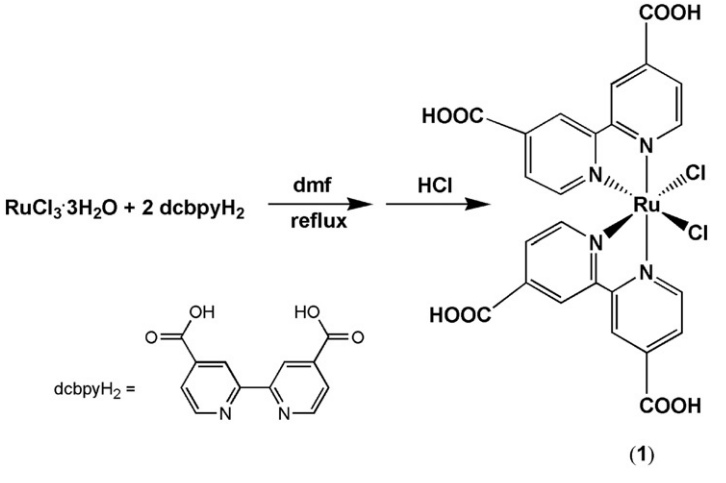

Scheme 2. Synthesis of *cis*-[Ru(dcbpyH$_2$)$_2$Cl$_2$] (**1**).

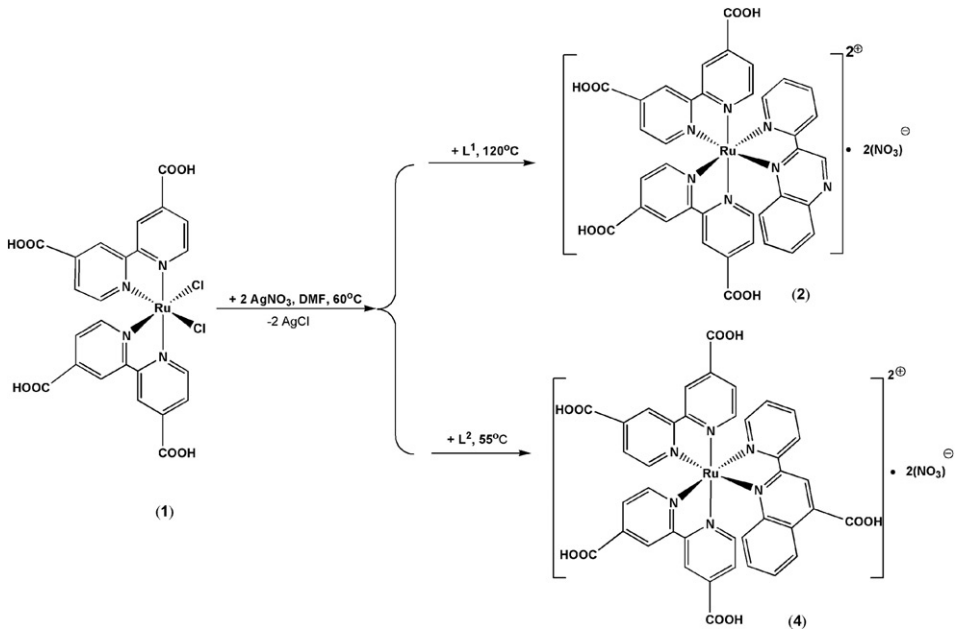

Scheme 3. Synthetic procedure of **2** and **4** starting from **1**.

decompose at 215°C and 200°C, respectively [22]. During the preparation of both compounds, $[Ru(dcbpyH_2)_3]Cl_2$ (**3**) was isolated as a side product [23].

Compounds **2** and **4** were soluble in water, methanol, and ethanol, and less soluble in DMSO and DMF. Spectroscopic characterization of the two compounds was performed by FT-IR, FT-Raman, UV-Vis, ^1H, ^{13}C NMR spectroscopy and by 2-D H–H COSY, H–C HSQC, H–H NOESY, and H–H ROESY experiments. Molecular compositions were confirmed by electrospray mass spectrometry (ESI-MS) in MeOH. The main peaks that were detected at $m/z = 398.6$ (**2**) and at $m/z = 420.0$ (**4**) corresponding to the dicationic molecular ion ($\{M/2\}^{2+}$). In all cases, the mass distribution within each cluster of peaks owing to isotopic diversity was well matched by computed spectra. Finally, the formulas were also confirmed by elemental analyses. Despite repeated crystal growth attempts with the two new complexes, only microcrystals or powders were obtained.

The structures of **2** and **4** are analogous to other Ru(II) compounds that exhibit interesting biological activity (such as DNA binding and/or intercalation) and potential anticancer properties [11, 12, 14]. Thus, the interaction of these Ru(II) polypyridyl complexes with DNA has attracted considerable attention and it has been proven that DNA binding affinities depend on both ligands and ligand substituents [24]. The octahedral $[Ru(bpy)_2(L^1)]^{2+}$ has been reported to interact with the major groove close to the T8C9 sequence within the oligonucleotide $d(CGCGAATTCGCG)_2$ [25]. Compared to the latter, *cis*-$[Ru(dcbpyH_2)_2(L^1)](NO_3)_2$, **2**, displays a very similar molecular structure, containing the same L^1, while two carboxylic acid groups (−COOH) have displaced hydrogen in the 4,4′ positions of bpy. For **4**, the presence of one −COOH group in the pyridyl ring instead of a nitrogen atom in **2** should interfere with its biological activity. $[Ru(terpy)(dcbpyH_2)Cl]Cl$ incorporating $dcbpyH_2$ has been

recently screened as an antiproliferation metallodrug [26]. Furthermore, $[Ru(dmb)_2(pdpt)](ClO_4)_2$ (dmb = 4-dimethyl-2, 2-bipyridine pdpt = 3-(pyridine-2-yl)-5,6-diphenyl-as-triazine) [27] and $[Ru(dmp)_2(APIP)](ClO_4)_2$ (APIP = 2-(2-aminopheny-limidazo[4,5-f][1,10]phenanthroline), dmp = 2,9-dimethyl-1,10-phenanthroline) [28] revealed partial intercalation, with π-stacking on the DNA surface and interaction with DNA through intercalation. The former is an effective antioxidant against hydroxyl radical ($^{\bullet}OH$) showing DNA photo-cleavage properties while cytotoxicity of the latter was demonstrated in a series of cell lines. For $[Ru(dmb)_2(pdpt)](ClO_4)_2$ and $[Ru(dmp)_2(APIP)](ClO_4)_2$, these are doubly charged as the relevant complexes described here with the coordination sphere around ruthenium constituted by substituted bpy and phenanthroline groups that show analogous behavior to $dcbpyH_2$ present in **2** and **4**. The basic core of pdpt is mainly constituted from a substituted bpy functionalized with two other pyridyl moieties rather than one in the case of L^1 (**2**) and L^2 (**4**). APIP comprises a phenanthroline core extended by a pyrazol in conjunction to a pyridyl amine group. The above discussion clearly demonstrates that research in the field of bioinorganic chemistry and the seek for new metal-based drugs are very important research topics of continuous interest. According to similarities in the structural features of the previously mentioned ruthenium analogues and the complexes described in this article, encouraging biological action of **2** and **4** is expected. These octahedral coordination compounds are inert to substitution and suitable for interaction with DNA. The above properties suggest potential future use as components of anticancer drugs and for this reason the cytotoxicity of both compounds toward a range of cell lines merits investigation.

3.2. *Characterization*

3.2.1. IR-Raman spectroscopic data. IR spectra of **2** and **4** are almost identical from 4000 to 400 cm^{-1}, as expected for compounds that have similar molecular structures. Both complexes exhibit a broad and medium intensity absorption at 1719 and 1718 cm^{-1}, respectively, assigned to ν(C=O) (at 1718 cm^{-1} for **3**). Bands at 1618 (**2**), 1611 (**3**), and 1616 (**4**) cm^{-1}, respectively, overlapping with the bpy bands, are tentatively assigned to the antisymmetric carboxylate $\nu_{as}(CO_2^-)$ [29], while ν(C–O) is present in each complex as a medium intensity band at 1232 cm^{-1}. The very strong and intense broad band at 1385 cm^{-1} [30] can be readily assigned to the anti-symmetric stretching mode (ν_3) of nitrate [31]. This band is shifted to higher wavenumbers compared to that of nitrate in $AgNO_3$ (ν_3 at 1378 cm^{-1}, in nujol) and in KNO_3 (ν_3 at 1370 cm^{-1}). In the FT-IR spectrum of **2**, the in-plane and out-of-plane pyridine-ring bands at 620 and 401 cm^{-1} in the free ligand (L^1) [16] are shifted to 670 and 454 cm^{-1}, respectively, indicating coordination to Ru(II) through the pyridyl nitrogen.

Complexes **2** and **4** exhibit resonance-enhanced Raman spectra under 514.5 nm excitation, which approaches their highest wavelength absorption maxima (vide infra in the electronic spectra section), in contrast to the very weak intensity of the Raman spectra at 785 nm (not shown) impeded by strong luminescence. Both complexes show a series of intense, well-resolved Raman bands at 1000–1700 cm^{-1} (figure 1), indicative of the high purity and crystallinity of the compounds.

The C=O stretch is identified at 1719 cm^{-1} for **4**, whereas it is hardly discernible for **2**. A double peak is observed at high wavenumbers (1600 and 1614 cm^{-1}) arising

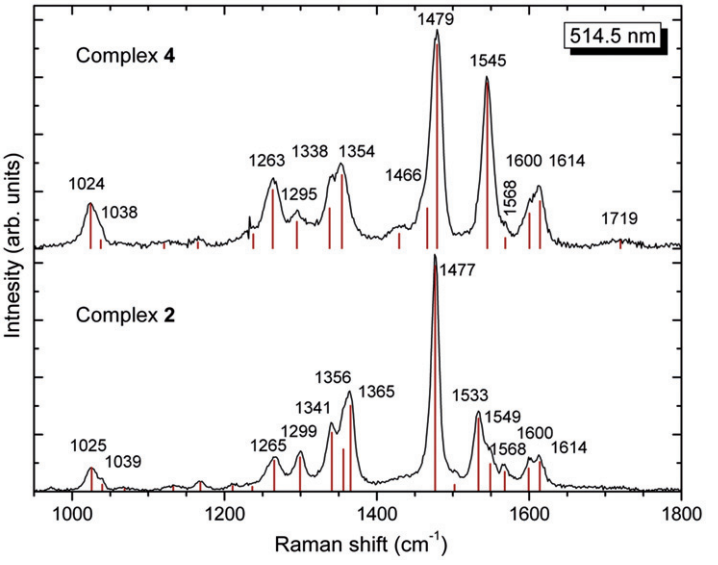

Figure 1. Micro-Raman spectra of **2** and **4** in powder form at 514.5 nm.

from the distinct Raman modes of the constituent ligands, similar to other heteroleptic polypyridyl Ru complexes [32]. Specifically, the band at 1600 cm^{-1} can be assigned to the highest wavenumber pyridine ring stretching mode, as previously reported for homologous complexes with the metal coordinated to L^2 [17], terpyridine [33], or 2-(2′-pyridyl)quinoxaline) (L^1) [34], while the band at 1614 cm^{-1} can be identified with the corresponding mode of $dcbpyH_2$ [17, 35]. Substitution of the carboxylic acid group of L^2 with nitrogen (L^1) in the central pyridine results in the splitting of the dominant ring stretching mode at 1545 cm^{-1} (**4**) to two weaker modes at 1533 and 1549 cm^{-1} (**2**), in agreement with previous Raman data on transition metal complexes containing 2-(2′-pyridyl)quinoxaline) [15]. The different coordinating ligands can be further discriminated by the composite band at ~1350 cm^{-1} that is characteristic of the inter-ring vibrations in polypyridyl complexes of L^1 or L^2, while absent in $dcbpyH_2$.

3.2.2. NMR spectroscopy. NMR spectroscopy verified the identities of the new complexes. ^1H NMR spectra of **2** and **4** are quite complicated and signal assignment was based on integration, splitting patterns, chemical shifts, and mainly on a combination of two-dimensional experiments. In any case their ^1H NMR spectra are in agreement with the proposed molecular structures. The characteristic ^1H NMR spectrum of **2** was recorded in the D_2O solution containing 0.05 mol L^{-1} NaOD and is illustrated in figure 2. The aromatic region of the spectrum displays sharp and well-resolved peaks, respectively, attributed to the protons of the two non-equivalent $dcbpyH_2$ ligands and of the 2-(2′-pyridyl)quinoxaline ligand (L^1). Thus, the intense single resonance at 9.76 ppm is typical for the H_3 proton of the quinoxaline ligand that is uncoupled. In the 2-D NOESY NMR experiment cross peaks between H_3–H_{13}, H_{19}–$H_{19'}$, and H_9–$H_{22'}$ were observed, revealing connectivity between the

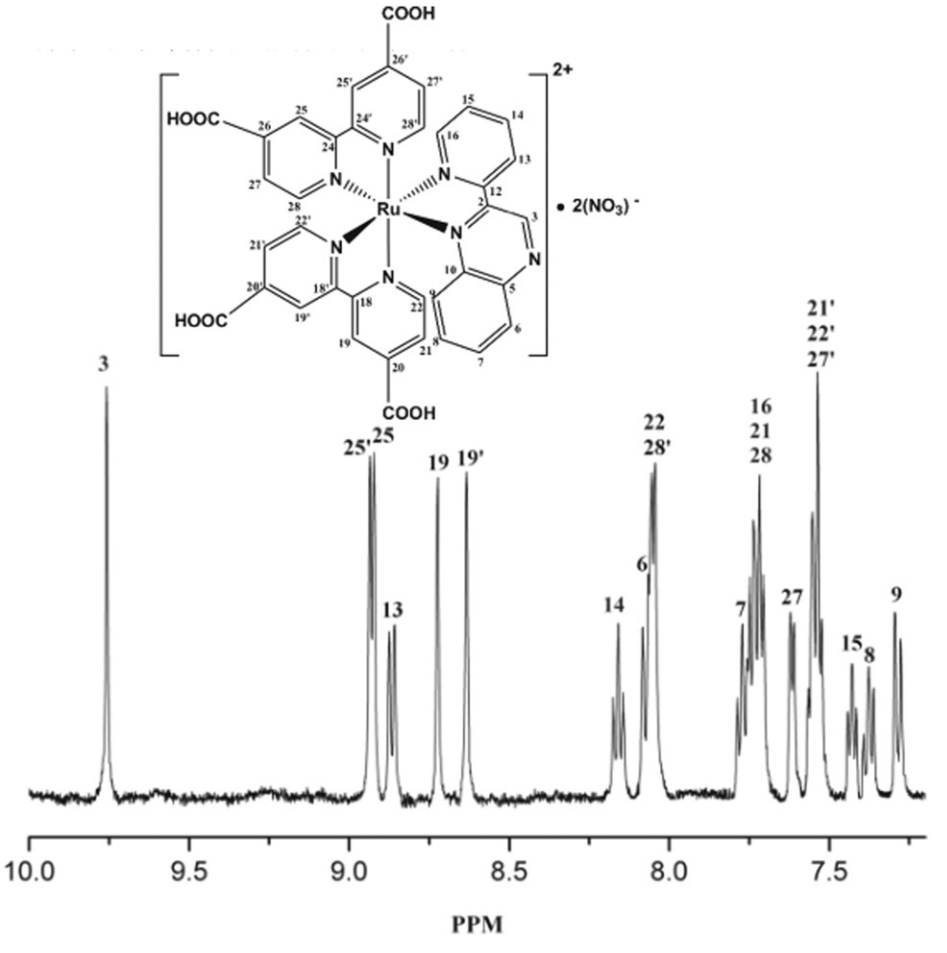

Figure 2. ^{1}H NMR spectrum of *cis*-[Ru(dcbpyH$_2$)$_2$(L^1)](NO$_3$)$_2$ (**2**) in D$_2$O containing NaOD 0.05 mol L^{-1} at an ambient temperature. A numbering scheme showing our tentative assignment for NMR peaks is included.

corresponding pyridyl and quinoline units. The remaining protons were assigned with the aid of H,C-HSQC experiments as well.

The ^{1}H NMR spectrum of **4** (in the aromatic region) exhibits the expected distinct resonances due to the presence of dcbpyH$_2$ while the chemical shifts of H$_{22}$ and H$_{28}$ are too close with the δ values of H$_{14}$ and H$_{16}$ of L^2. The NMR spectral data of **1**–**4** are collected in table 1. Substitution of the two chlorides by L^1 or L^2 influences the chemical shift values of H$_6$ ($\delta = 9.84$ ppm) and H$_5$ ($\delta = 8.13$ ppm) in the *o*- and *m*-positions of dcbpyH$_2$ in **1**. As a result, these protons are shifted upfield by 2.09 and 2.30 ppm (H$_{28,22'}$) and by 0.51 and 0.59 ppm (H$_{27,21'}$) and appear as doublet and doublet of doublets.

After the coordination of L^1 or L^2 to ruthenium(II) and due to electronic surroundings H$_{25'}$, H$_{19}$, H$_{28'}$, H$_{27'}$, H$_{22}$, and H$_{21}$ of dcbpH$_2$ at axial position are downfield shifted compared to the equatorial H$_{25}$, H$_{19'}$, H$_{28}$, H$_{27}$, H$_{22'}$, and H$_{21'}$ [36]. The ^{13}C NMR signals of **2** and **4** were assigned by 2-D HSQC experiments and

Table 1. ^{1}H-NMR chemical shifts (δ, ppm) of the 2,2′-bipyridine-4,4′-dicarboxylic acid ligand ($dcbpyH_2$) and of **1–4** in the D_2O solution containing 0.05 mol L^{-1} NaOD.

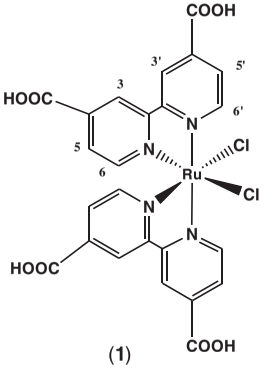

(1)

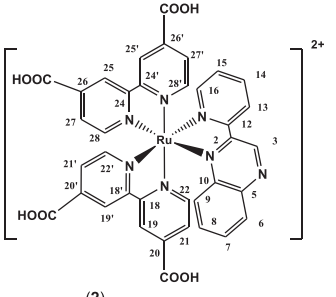

(2)

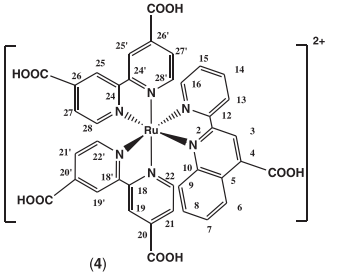

(4)

Compounds	H_6($^{b}_{28,22'}$)	$H_{6'}$($^{b}_{28',22}$)	H_5($^{b}_{27,21'}$)	$H_{5'}$($^{b}_{27',21}$)	H_3 ($^{b}_{25,19'}$)	$H_{3'}$ ($^{b}_{25',19}$)
$dcbpyH_2$	8.78(d)	–	7.87(dd)	–	8.40(d)	–
1[a]	9.84(d)	7.80(d)	8.13(dd)	7.39(dd)	8.86(d)	8.69(d)
2[b]	7.75(m),	8.06(m)	7.62(d),	7.54(m),	8.92(s),	8.94(s),
	7.54(m)		7.54(m)	7.75(m)	8.63(s)	8.72(s)
3	7.81(d)	–	7.61(d)	–	8.81(s)	–
4[b]	7.65(d),	8.10(m),	7.57(m)	7.57(m),	8.95(s),	8.98(s),
	8.27(d)	7.76(d)		7.72(d)	8.59(s)	8.69(m)

[a]After a few minutes, new resonance signals next to the expected ones appear which are shifted upfield compared to that of freshly prepared samples.
[b]Proton numbering of the $dcbpyH_2$ ligands in **1–4** is given in the upper part of the table.

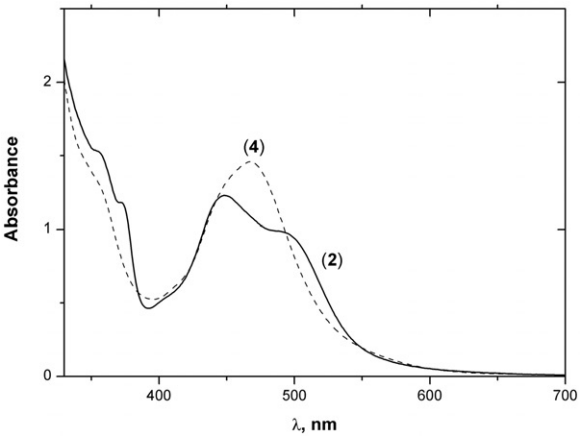

Figure 3. Absorption spectra of **2** and **4** in methanol (10^{-5} mol L^{-1}).

Table 2. Electronic spectroscopic data of **2–4** in methanol at 298 K.

Complexes	Absorption data [λ_{max} (nm) (ε, 10^4 mol^{-1}L^{-1}cm^{-1})]				
1	314 (3.5)	403 (9.3)	–	–	550 (9.1)
2	307 (5.6)	351 (1.7)	369 (1.3)	448 (1.4)	491 (1.1)
3[a]	308 (7.0)	353 (1.8)	–	440 (1.6)	470 (2.0)
4	307 (7.0)	344 (1.6)	–	–	466 (1.6)

[a]In aqueous 1 mol L^{-1} HCl solution.

comparison with the literature data [37]. The typical ^{13}C-{^{1}H} NMR spectrum of **2** in the aromatic region ($\delta = 122$–170 ppm) presents the expected resonances corresponding to the pyridyl ring carbons. The four resonances at 170.20, 170.08, 170.04, and 169.97 ppm are assigned to carbons of the four carboxylic acid groups. For **4**, the low-field resonances at $\delta = 173.00$, 170.47, 170.31, 170.25, and 170.22 ppm are due to carbons of the five carboxyl groups.

3.2.3. Electronic spectra. Absorption spectra of a methanol solution of *cis*-[Ru(dcbpyH$_2$)$_2$(L^1)](NO$_3$)$_2$ (**2**) and *cis*-[Ru(dcbpyH$_2$)$_2$(L^2)](NO$_3$)$_2$ (**4**) are shown in figure 3. The electronic spectroscopic data of the two complexes including **3** (in aqueous 1 M HCl) and the starting material **1** are summarized in table 2. Spectroscopic data reveal that upon the substitution of chlorides from **1**, absorption spectra of **2** and **4** features characteristic absorptions that are blue shifted [38]. Complex **2** displays a rather broad absorption consisting of two overlapping bands with maxima at 491 ($\varepsilon = 1.1 \times 10^4$) and 448 nm ($\varepsilon = 1.4 \times 10^4$ (mol L^{-1})$^{-1}$ cm^{-1}) assigned to ^{1}MLCT absorptions, as expected for Ru(II) polypyridyl complexes [39]. The visible spectrum of **4** bearing the 4-carboxy-2-(2′-pyridyl)quinoline is dominated by a broad band centered at 466 nm ($\varepsilon = 1.6 \times 10^4$ (mol L^{-1})$^{-1}$ cm^{-1}). This could be compared with the absorption maximum (λ_{max}) at 452 nm observed for *cis*-[Ru(bpy)$_2$(L^2)]Cl$_2$ [6f]. Molar extinction

coefficient (ε) values of **2** and **4** are of the same order of magnitude as *cis*-[Ru(dcbpyH)$_2$(NCS)$_2$](NBu$_4$)$_2$ **N719** dye ($\varepsilon = 1.4 \times 10^4 (\text{mol L}^{-1})^{-1}\text{cm}^{-1}$) [40]. This is very promising for the application of these mononuclear complexes in the fabrication of photovoltaic devices based on DSSCs technology, as evidenced from the photovoltaic performance of a solar cell incorporating dye **4** that displays a solar energy to electricity efficiency (η) of 1.58% [41]. The power conversion efficiency of **4** is significantly higher than for *cis*-[Ru(bpy)$_2$(L^2)]Cl$_2$ ($\eta = 0.03\%$) [6f], but is of the same order of magnitude as *cis*-[Ru(dcbpyH$_2$)$_2$(α-CD-5-bpy)]Cl$_2$ (α-CD-5-bpy = 6-mono[5-methyl(5′-methyl-2,2′-bipyridyl)]-permethylated α-CD; CD = cyclodextrin) [6e] revealing the importance of the bidentate dcbpyH$_2$ on the performance of the corresponding DSSC. Power conversion efficiencies (η) as low as 0.013% were obtained on cells fabricated using the [tdctpyRu-(idctpy)][PF$_6$]$_2$ sensitizer (tdctpy = 4′-p-tolyl-4,4″-dicarboxy-2,2′: 6,2″-terpyridine, and idctpy = 4′-*p*-iodophenyl-4,4″-dicarboxy-2′: 6,2″-terpyridine) bearing carboxy-functionalized tridentate ligands [42].

4. Conclusions

In this article we have demonstrated that the substitution of *cis*-[Ru(dcbpyH$_2$)$_2$Cl$_2$] (**1**) with 2-(2′-pyridyl)quinoxaline (L^1) and 4-carboxy-2-(2′-pyridyl)quinoline (L^2) in the presence of silver(I) salts leads to cationic complexes *cis*-[Ru(dcbpyH$_2$)$_2$(L^1)](NO$_3$)$_2$ (**2**) and *cis*-[Ru(dcbpyH$_2$)$_2$(L^2)](NO$_3$) (**4**). The new heteroleptic Ru(II) compounds were obtained pure and fully characterized by a combination of spectroscopic methods. The experimental results confirm the proposed structure for the octahedral ruthenium(II) complexes. Application of the new coordination compounds in biological systems could be envisaged given their structural analogy with known ruthenium(II) polypyridine complexes that are in medical or clinical use. Complexes **2** and **4** are expected to interact with DNA, while investigation of the anticancer activity of the new components might contribute further in this field.

Both complexes display high molar extinction coefficients that are comparable to those of **N719** dye. Although their photovoltaic performance is not equivalent to that of **N719**, their sensitizing ability compares well to that of related complexes bearing carboxy-functionalized tridentate ligands, thus denoting the importance of the bidentate anchoring dcbpyH$_2$ in the coordination sphere of the dye molecular compounds. Based on these results, judicious design and development of new light molecular antennas is underway, rendering them candidates for the fabrication of highly performing photovoltaic devices based on DSSCs technology.

Acknowledgments

A. Philippopoulos thanks "The Special Research Account of National and Kaposistrian University of Athens" for financial support (Kapodistrias program number 70/4/9277) and E. Chatzivasiloglou thanks the NCSR "Demokritos" for fellowship allowance. P. Falaras greatly acknowledges financial support from the General Secretariat for Research and Development (GSRT – Greece) through 03ED

118/2005 "PENED" project. The authors express their gratitude to Dr L. Leontiadis (Dioxin Analysis Lab/NCSRD) for the ESI-MS measurements.

References

[1] J.G. Vos, J.M. Kelly. *Dalton Trans*., 4869 (2006).
[2] V. Balzani, A. Juris, M. Venturi, S. Campagna, S. Serroni. *Chem. Rev*., **96**, 759 (1996).
[3] J.P. Paris, W.W. Brandt. *J. Am. Chem. Soc*., **81**, 5001 (1959).
[4] (a) M. Grätzel. *Acc. Chem. Res*., **42**, 1788 (2009). (b) G.J. Meyer. *ACS Nano*, **4**, 4337 (2010).
[5] M. Grätzel. *J. Photochem. Photobiol. A*, **164**, 3 (2004).
[6] (a) A. Hagfeldt, G. Boschloo, L Sun, L. Kloo, H. Pettersson. *Chem. Rev*., **110**, 6595 (2010); (b) J.N. Clifford, E. Martínez-Ferrero, A. Viterisi, E. Palomares. *Chem. Soc. Rev*., **40**, 1635 (2011); (c) F.A. Almutlaq, P.G. Potvin, A.I. Philippopoulos, P. Falaras. *Eur. J. Inorg. Chem*., 2121 (2007); (d) A.I. Philippopoulos, A. Terzis, C.P. Raptopoulou, V.J. Catalano, P. Falaras. *Eur. J. Inorg. Chem*., 5633 (2007); (e) J. Faiz, A.I. Philippopoulos, A.G. Kontos, P. Falaras, Z. Pikramenou. *Adv. Funct. Mater*., **17**, 54 (2007); (f) G. Konti, E. Chatzivasiloglou, V. Likodimos, G. Kantonis, A.G. Kontos, A.I. Philippopoulos, P. Falaras. *Photochem. Photobiol. Sci*., **8**, 726 (2009).
[7] (a) H. Doucet, T. Ohkuma, K. Murata, T. Yokozawa, M. Kozawa, E. Katayama, A.F. England, T. Ikariya. *Angew. Chem. Int. Ed*., **37**, 1703 (1998); (b) M.P. Araujo, A.T. Figuiredo, A.L. Bogado, G. Poelhsitz, J. Ellenea, E.E. Castellano, C.L. Donnici, J.V. Comasseto, A.A. Batista. *Organometallics*, **24**, 6159 (2005); (c) M. Aydemir, A. Baysal. *Polyhedron*, **29**, 1219 (2010).
[8] R.A. Sheldon, I.W.C.E. Arends, Gerd-Jan ten Brink, A. Dijksman. *Acc. Chem. Res*., **35**, 774 (2002).
[9] H.S. Ahn, S.H. Han, S.J. Uhm, W.K. Seok, H.N. Lee, G.A. Korneeva. *J. Mol. Catal. A-Chem*., **144**, 295 (1999).
[10] (a) R. Noyori, T. Ohkuma. *Angew. Chem. Int. Ed*., **40**, 40 (2001); (b) J.E. Bäckvall. *J. Organomet. Chem*., **652**, 105 (2002); (c) A.I. Philippopoulos, E. Kolovou, N.G. Tsierkezos, A. Paulidou, I.M. Mavridis, S. Batistatou, E. Bakeas. *Global J. Inorg. Chem*., **2**, 92 (2011).
[11] (a) L. Herman, S. Ghosh, E. Defrancq, A. Kirsch-De Mesmaekera. *J. Phys. Org. Chem*., **21**, 670 (2008). (b) A. Ambroise, B.G. Maiya. *Inorg. Chem*., **39**, 4264 (2000).
[12] F. Gao, H. Chao, Y.-F. Wei, Y.-X. Yuan, B. Peng, X. Chen, K.-C. Zheng, L.-N. Ji. *Helv. Chim. Acta*, **91**, 395 (2008).
[13] A.E. Friedman, J.C. Chambron, J.P. Sauvage, N.J. Turro, J.K. Barton. *J. Am. Chem. Soc*., **112**, 4960 (1990).
[14] (a) M.J. Clarke. *Coord. Chem. Rev*., **232**, 69 (2002). (b) A.R. Timerbaev, C.G. Hartinger, S.S. Aleksenko, B.K. Keppler. *Chem. Rev*., **106**, 2224 (2006). (c) W.H. Ang, P.J. Dyson. *Eur. J. Inorg. Chem*., 4003 (2006). (d) P. Nowak-Sliwinska, J.R. van Beijnum, A. Casini, A.A. Nazarov, G. Wagnieres, H. van den Bergh, P.J. Dyson, AW. Griffioen. *J. Med. Chem*., **54**, 3895 (2011).
[15] A.I. Philippopoulos, N. Tsantila, C.A. Demopoulos, C.P. Raptopoulou, V. Likodimos, P. Falaras. *Polyhedron*, **28**, 3310 (2009).
[16] S. Kasselouri, A. Garoufis, A. Katehanakis, G. Kalkanis, S.P. Perlepes, N. Hadjiliadis. *Inorg. Chim. Acta*, **207**, 255 (1993).
[17] Y. Bass, R.J. Morgan, R.J. Donovan, A.D. Baker. *Synth. Commun*., **27**, 2165 (1997).
[18] M.K. Nazeeruddin, M. Grätzel. *Inorg. Synth*., **33**, 185 (2002).
[19] S.M. Zakeeruddin, Md.K. Nazeeruddin, R. Humphry-Baker, M. Grätzel. *Inorg. Chim. Acta*, **296**, 250 (1999).
[20] The direct reaction of staring material **1** with L^1 in DMF at 155°C for 20 h was accompanied by decomposition of the starting material leading to a product, hard to be characterized. The corresponding ligand remained uncoordinated as it was evidenced by ^{1}H-NMR spectroscopy.
[21] Upon extended heating (from 70°C up to 120°C) the yield of **4** is decreased from 28 to 12%.
[22] The decomposition process was followed by IR spectroscopy (in KBr) revealing the gradual disappearance of the ν_{as}(C=O) stretching vibration of the −COOH group upon heating (vide infra, in the IR section). In fact, decarboxylation begins at 215°C and is completed at 250°C.
[23] The nature of the side product was identified on the basis of electrospray mass spectrometry and by comparison of its IR and NMR data (^{1}H, ^{13}C (1D and 2D) experiments) with those of an authentic sample: P.A. Lay, A.M. Sargeson, H. Taybe, *Inorg. Synth*., **24**, 291 (1986).
[24] Y. Liu, Y.-J Liu, J.-H. Yao, W.-J. Mei, F.-H. Wu. *J. Coord. Chem*., **62**, 1701 (2009).
[25] A. Garoufis, G. Malandrinos, N. Hadjiliadis. *Eur. J. Inorg. Chem*., 3326 (2004).
[26] Y.H. Wang, C.C. Cheng, W.J. Lee, M.L. Chiou, C.W. Pai, C.C. Wen, W.L. Chen, Y.H. Chen. *Chem. Biol. Interact*., **182**, 84 (2009).

[27] X.-L. Hong, Z.-H. Liang, M.-H. Zeng. *J. Coord. Chem.*, **64**, 3792 (2011).
[28] Z.-H. Liang, Z.-Z. Li, H.-L. Huang, Y.-J. Liu. *J. Coord. Chem.*, **64**, 3342 (2011).
[29] Md.K. Nazeeruddin, R. Humphry-Baker, P. Liska, M. Grätzel. *J. Phys. Chem. B*, **107**, 8981 (2003).
[30] A.F. Demirörs, B.E. Eser, Ö. Dag. *Langmuir*, **21**, 4156 (2005).
[31] K. Nakamoto. *Infrared and Raman Spectra of Inorganic and Coordination Compounds Part A: Theory and Applications in Inorganic Chemistry*, 5th Edn, John Wiley and Sons, Inc., New York (1997).
[32] G.D. Danzer, K. Bajdor, J.R. Kincaid. *J. Raman Spectrosc.*, **24**, 357 (1993).
[33] S. Schneider, G. Brehm, C.-J. Prenzel, W. Jäger, M.I. Silva, H.D. Burrows, S.T. Formosinho. *J. Raman Spectrosc.*, **27**, 163 (1996).
[34] M.R. Waterland, S.L. Howell, K.C. Gordon, A.K. Burrell. *J. Phys. Chem. A*, **109**, 8826 (2005).
[35] T. Stergiopoulos, M.-C. Bernard, A. Hugot-Le Goff, P. Falaras. *Coord. Chem. Rev.*, **248**, 1407 (2004).
[36] A.C.G. Hotze, J.A. Faiz, N. Mourtzis, G.I. Pascu, P.R.A. Webber, G.J. Clarkson, K. Yannakopoulou, Z. Pikramenou, M.J. Hannon. *J. Chem. Soc., Dalton Trans.*, **24**, 3025 (2006).
[37] In the ^{13}C NMR spectra, resonance signals from L^1 or L^2 were unfortunately overlapped with the corresponding signals belonging to the dcbpyH_2 ligand, making individual assignment impossible.
[38] W.K. Seok, A.K. Gupta, S.-J. Roh, W. Lee, S.-H. Han. *Bull. Korean Chem. Soc.*, **28**, 1311 (2007).
[39] A. Juris, V. Balzani, F. Barigelletti, S. Campagna, P. Belser, A. von Zelewsky. *Coord. Chem. Rev.*, **84**, 85 (1988).
[40] M. Grätzel. *Inorg. Chem.*, **44**, 6841 (2005).
[41] G.C. Vougioukalakis, A.I. Philippopoulos, T. Stergiopoulos, P. Falaras. *Coord. Chem. Rev.*, **255**, 2602 (2011).
[42] Y. Ou, G. Chen, J. Yin, G.-A. Yu, S.H. Liu. *J. Coord. Chem.*, **64**, 3062 (2011).